

Investigation of Combustion of the Gas Turbine Engine from Kerosene and Biokerosene and Their Soot Characteristics in Diffusion Flames

Thong D. Hong,* Iman K. Reksowardojo, Tatang H. Soerawidjaja, and Osamu Fujita



Cite This: *ACS Omega* 2022, 7, 37085–37094

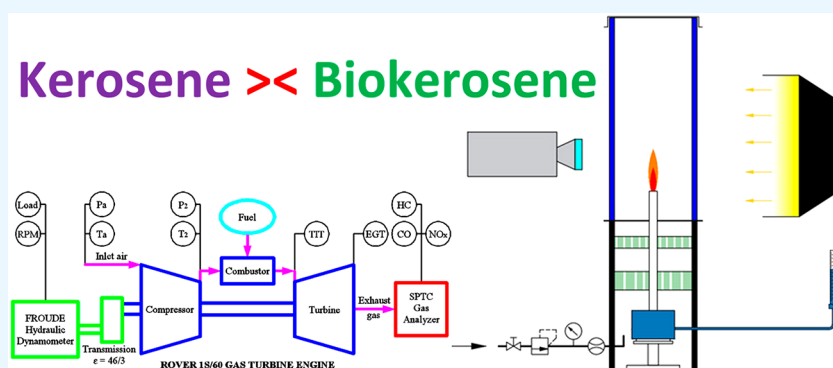


Read Online

ACCESS |

Metrics & More

Article Recommendations



ABSTRACT: Performances, emissions from the gas turbine engine, and soot formations in diffusion flames of kerosene (Jet A1) and its mixture with 5% by volume bioparaffins (known as BK-5) are reported in the present study. A Rover 1S/60 gas turbine engine was used for recording performance parameters and emissions. Soot characteristics were investigated in smoke-free coannular wick-fed diffusion flames. This study is the next step that must be performed in the certification process of a new aviation biofuel before it is tested in the aircraft. The results show that BK-5 produced a similar performance against Jet A1. Throughout the whole power range under investigation, BK-5 emitted 3.4% NO_x higher than Jet A1, while Jet A1 released CO and HC at the rates that are, respectively, 1.8 and 4.5% greater than its counterpart. The soot emissions from the BK-5 and Jet A1 were comparable across the measured flame height range. The results encouraged future studies to carry out the modern engine and flight tests. The production process for bioparaffins employed in this work has been demonstrated to be viable and appropriate for tropical developing nations. The current process should also continue to be improved by eliminating high-distillation temperature components in bioparaffins.

1. INTRODUCTION

The depletion of fossil-based fuels, international energy security, volatility of the global energy market, and negative environmental impacts have mainly concerned aviation policymakers and operators. Biofuels were a hopefully potential solution for all the above problems. Especially since the European Union Emissions Trading Scheme¹ has taken effect and been applied to the civil aviation sector since 2012, aviation biofuels have enjoyed a high level of interest with the participation of many researchers.

In the study by Liu et al.,² castor oil was hydroprocessed in a continuous-flow fixed-bed microreactor to create aviation biofuel with a high yield. They reported that the highest jet paraffin range yields of 91.6 wt% were obtained over nickel supported on acidic zeolites with a high isomer/n-alkane ratio. Tian et al.³ presented an atom-economic method for converting oleic acid into the range of hydrocarbons and aromatics used in aviation fuel without needing a hydrogen donor. Under the ideal

reaction conditions, oleic acid can be in situ hydrogen transferred, aromatized, and decarboxylated to yield 71% heptadecane and 19% aromatics. Wang et al.⁴ used metabolically engineered *Escherichia coli* to biosynthesize medium-chain length alkanes for biojet fuel. The findings demonstrated that thioesterase could adjust the chain length of the fatty acid in a carbon range acceptable for usage as feedstock for aircraft fuel. Reactive distillation columns were used in the work of Gutiérrez-Antonio and co-workers⁵ to intensify the hydrotreating process using the *Jatropha Curcas* oil as a renewable raw resource. The results demonstrated that this intensification technique

Received: May 1, 2022

Accepted: September 28, 2022

Published: October 12, 2022



increases biojet fuel yield while reducing operating pressure and environmental effect. Araújo et al.⁶ used a 5% Pd/C catalyst in a semibatch reaction to produce n-alkanes with up to 39.2% conversion. The decarboxylation pathway is preferred, as shown by the n-alkane selectivity of 80.7% and the CO₂ selectivity of 83.4% for biodiesel, which also validates Licuri as a possible feedstock for biojet fuel.

Duong et al.⁷ developed a soap-derived biokerosene (SBK) production process, which consisted of two basic procedures of saponification and thermal decarboxylation. According to the findings, SBK can be blended directly with Jet A1 at 10% volume to meet the jet fuel standard ASTM D1655. In the study of da Silva et al.,⁸ methanol was used to transesterify oil from the kernels of macaúba and palm using the traditional reaction with a homogeneous alkaline catalyst. To create enriched fractions in light biodiesels, the carbon number from 8 to 14 was selected, and the fatty acid methyl esters were further distilled. The work presented that the light biodiesels may be blended with Jet A1 up to a minimum of 5% volume was met the ASTM D1655. The physicochemical properties of reproductive materials from *Pongamia* trees growing under various conditions at five separate sites on the island of Oahu in Hawaii were studied by Fu et al.⁹ *Pongamia* oil was discovered to share traits with canola and *Jatropha* seed oils, and it would be predicted to be well adapted for hydroprocessing production of sustainable aviation fuel; however, pods would need additional processing before being used as fuel because of their high potassium and chlorine levels. Donoso et al.¹⁰ compared hydrogenated turpentine at various levels of conversion with turpentine obtained by vacuum distillation of resin obtained from the common pine *Pinus pinaster* or as the paper industry byproduct. It was concluded that partially hydrogenated turpentine could be blended up to 50% by volume with Jet A1, meeting the standard requirement for aviation biofuels. Li et al.¹¹ have created high-energy biofuels using engineered intermediates that considerably impact their reactivity with various biomass feedstocks when used in single-pot, two-pot, or solvent-free reactions. A variety of bi-(cyclopentane)-based alkanes can be synthesized selectively with high to exceptional overall isolated yields of 68–90%.

The development of biofuel for the aviation industry depends on the circumstances of each country, such as social and economic position, science and technology levels, feedstock sources, climate, and soils. Countries with different conditions can choose different ways to develop their aviation biofuel. However, candidates for alternative fuel use in aircraft engines must undergo a thorough testing process in laboratories, on-ground equipment, and under extreme operating conditions to meet safety requirements. Specifications of the testing process of aviation biofuel meet the requirements of the ASTM D4054 standard.¹²

As soon as they are generated, the aviation biofuels are evaluated according to their specifications, including distillation points, flash point, density, freezing point, viscosity, net heat of combustion, smoke point, vapor pressure, acidity, aromatics, sulfur, thermal stability, and so on. These biofuels are blended with conventional aviation fuels in different proportions to determine their compliance with the ASTM standard, which has been demonstrated in published studies.^{6–11} In addition, many studies have addressed biofuel's soot emissions because of their significant and critical impacts on engines, human health, and the environment.

Duong et al.¹³ investigated the freezing point, smoke point, and total soot volume of dodecane, SBK, and their blends with

butyl-cyclohexane and butyl-benzene. The authors reported that when blending with SBK or dodecane, butyl-cyclohexane significantly lessens the soot formation than butyl-benzene. In contrast, butyl-cyclohexane lowers the freezing point more than butyl-benzene. Kumal et al.¹⁴ evaluated the soot samples taken from the exhaust pipe of a J-85 turbojet powered by Jet A and blends of Jet A and *Camelina* biofuel using transmission electron microscopy analysis. The results emphasized critical points about utilizing biofuel instead of conventional aircraft fuel to reduce soot emissions and protect the environment and human health. The research of Andrade-Eiroa et al.¹⁵ aimed to shed light on the combustion mechanisms and assess the environmental impact of these synthetic biofuels by characterizing the polar aromatic compounds (PACs) adsorbed on soot produced in premixed flames of Jet A1, synthetic paraffinic kerosene, and Jet A1/synthetic biofuels (2, 5-dimethylfuran, 1-butanol, diethyl-carbonate, and methyl-octanoate). The emission of aromatic hydrocarbons was reduced when fossil fuels were blended with synthetic biofuels, except for 2, 5-dimethylfuran, but PAC production increased. Chang et al.¹⁶ examined how Chinese conventional jet fuel (RP-3) and aviation biofuels derived from algae changed the soot's morphology in free jet laminar diffusion flames. The authors found that biofuel particles are smaller than RP-3 particles in size. The primary soot particles of biofuel and RP-3 are 15.6 and 22.7 nm, respectively.

In a previous study,¹⁷ we proposed the production process of aviation biofuel for tropical countries. It was built on the hydrotreating process, and the feedstocks had to be chosen from medium-chain and dominating lauric fatty acids found in large quantities in coconuts and palm kernels. The manufacturing process appears to be the most straightforward, lowering investment and production costs. Additionally, it can partially utilize the biodiesel production line that is already in place. The bioparaffin prototypes, named Bio-P1 and Bio-JP2, were blended with Jet A1 with proportions up to 5 and 10% volume for making biokerosene that satisfied the ASTM D1655. In addition, soot formations of the bioparaffins, dodecane, and their mixtures with variable levels of propyl-benzene of 10, 20, and 25 vol % were determined and compared to each other, which are also presented in our previous work.¹⁸ Dodecane and propyl-benzene were selected as reference fuels because they are common aviation fuel surrogates for the paraffin and aromatic classes, respectively. The study reported that the aviation bioparaffins are highly comparable to dodecane in soot formation.

As the next step in the research and development of aviation biofuel, the performance and emissions of a turbine engine for kerosene (Jet A1) and its blend with 5% by volume aviation biofuel were investigated in the present study. Soot characteristics of these two fuels were also determined and compared in smoke-free coannular wick-fed diffusion flames. Numerous studies on biofuel combustion in gas turbine engines have been published; however, they are primarily for industrial applications rather than aviation. Another problem is that the author has little understanding of the bioparaffins utilized in this study because they were made using a different method from the standard ones now on the market. This study aims to identify and get insight into the effects of aviation biofuel on the performance and emissions of the turbine engine, as well as its soot formation in the diffusion flames when blended with fossil kerosene. The results of this work are being used to support upcoming flight

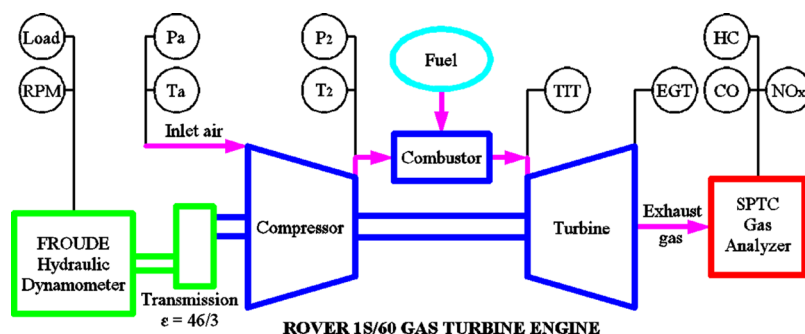


Figure 1. Schematic diagram of the experimental setup for performance and emission tests.

tests and study improvements in the manufacturing process of aviation biofuels.

2. EXPERIMENTAL SYSTEMS

2.1. Experimental Setup for Testing Performances and Emissions of the Gas Turbine Engine. Figure 1 presents the diagram for testing performances and emissions in the current study. A Rover 1S/60 gas turbine engine, which has a maximum continuous brake power of 44 kW (60 HP) at 46,000 rpm, was used. A Froude hydraulic dynamometer (made in England) was coupled with the turbine engine through a transmission for measuring load and speed. The maximum brake power of the dynamometer is 150 HP at 4000–7500 rpm, and the transmission ratio is 46/3. Exhaust gas emissions of HC, CO, and NO_x were recorded using a SPTC Gas & Smoke analyzer. The brief specifications of the turbine engine, measuring apparatuses, and exhaust gas analyzer are shown in Tables 123, respectively.

Table 1. Brief Specifications of the Rover 1S/60 Turbine Engine

| engine parameters or parts | value or type |
|----------------------------|--|
| compressor | centrifugal/single stage |
| turbine | axial/single stage |
| combustion chamber | single can with simplex burner nozzle/reverse flow |
| governed speed | 46,000 rpm |
| pressure ratio | 2.8:1 |
| Max. EGT | 580 °C |
| Max. power (46,000 rpm) | 44 kW at 580 °C EGT and 15 °C AIT |

Table 2. Specifications of Measuring Apparatuses

| measuring apparatus | parameter | range | accuracy |
|------------------------|--|-------------------|----------------|
| thermometer | air inlet temperature, T_a | 0–110 °C | ±1 °C |
| thermometer | compressor delivery temperature, T_2 | 80–250 °C | ±1 °C |
| thermometer | turbine inlet temperature, TIT | 300–900 °C | ±5 °C |
| thermometer | exhaust gas temperature, EGT | 250–800 °C | ±5 °C |
| manometer | air depression, P_a | 0–760 mm paraffin | ±1 mm paraffin |
| Bourdon pressure gauge | compressor delivery pressure, P_2 | 0–4 bar | ±0.025 bar |
| tachometer | brake speed, rpm | 0–5000 rpm | ±25 rpm |
| spring balance | load | 0–50 lb | ±0.2 lb |
| stopwatch | time to consume fuel | 0–99 min | ±0.01 s |

Table 3. Specifications of the SPTC Gas and Smoke Analyzer

| measurement | range | resolution | measuring method |
|-----------------|--------------|------------|------------------------|
| NO _x | 0–5000 ppm | 1.0 ppm | electrochemical cell |
| CO ₂ | 0–20% | 0.01% | nondispersive infrared |
| CO | 0–10% | 0.001% | nondispersive infrared |
| HC nhexane | 0–30,000 ppm | 1.0 ppm | nondispersive infrared |
| HC propane | 0–60,000 ppm | 1.0 ppm | nondispersive infrared |
| O ₂ | 0–25% | 0.01% | electrochemical cell |

The fuel consumption was determined by measuring the time that a given fuel volume was consumed. From these parameters, brake-specific fuel consumption was calculated. The engine was also equipped with the other apparatuses to observe air inlet temperature, compressor delivery temperature and pressure, the turbine inlet temperature (TIT), and exhaust gas temperature (EGT).

Jet A1 and its blend with 5% by volume aviation bioparaffins, known as BK-5, were used to power the turbine at various loads. The engine was run for at least 5 min on the chosen fuel for each test before performances and emissions were recorded. The tests were carried out at powers of about from 5 to 25 kW with an increment of around 2.5 kW. Each testing point was observed three times to produce the mean reading. All tests were conducted at ambient temperature and pressure.

2.2. Experimental Procedures for Investigations of Soot Characteristics. In the current study, the method for determining soot formation is similar to our previous work,¹⁸ in which the diagram of the experimental setup is provided in Figure 2. The light extinction measurements were used to determine the soot formations generated from the smoke-free coannular wick-fed diffusion flames. The wick's height was adjusted above the tube, which has an inner diameter of 7 mm, to control the flame height. The Pyrex glass is used to make the tubular combustor, which has an inner diameter and length of 90 and 250 mm, respectively.

For all tests, the air was delivered at a constant flow rate of 30 L per minute (approximately airflow velocity of 7.86 cm/s) from the bottom of the combustor. This value was generated based on the results of many previous experiments to produce stable flames across the investigating ranges of flame heights. The air was fed through two layers of honeycomb configuration, containing 750 cells/in² to provide a uniform flow field in the combustor. A flow restrictor, a stainless-steel bowl with a diameter of 120 mm, was put above the combustor to prevent air recirculation from generating a highly steady flame. The flow restrictor was made of a multihole design with a 6 mm diameter.

The wavelength for the extinction image was chosen using an interference filter lens, which only allows wavelengths of 540 nm

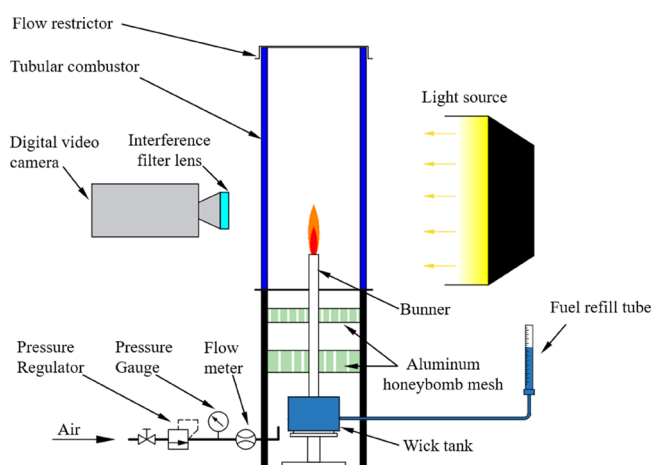


Figure 2. Schematic diagram of the experimental setup for investigations of soot characteristics.

to pass through it. The direction and shadow of the backlight were recorded using a digital camera with the filter lens installed. These recordings were converted to pictures, and then a MATLAB program was used to compare the light intensity of the stable flame pictures and the extinction pictures. The Bouguer–Beer–Lambert law was applied to determine the sooting characteristics. The experimental system was covered by the black-wall surroundings to prevent extraneous environmental impacts.

A digital balance's Shimadzu, a fuel refill injector, and a timer were used to measure the fuel mass consumption rate (FMCR). Each measurement of fuel mass consumption was made with a fuel mass greater than 1 g for increased accuracy. Each testing point was carried out three times to produce the mean reading, and each measurement has a 95% match in terms of repeatability. It indicates that the experimental data could be used to evaluate the FMCR measurement reliably.

FMCRs and total soot volumes (TSVs) were quantified in terms of flame heights for Jet A1 and BK-5. Then, the correlations between TSVs and FMCRs were found. Because of the presence of smoke in flames, the experiments were performed at a maximum flame height of 23 mm. All of the investigations were carried out at ambient pressure and temperature.

2.3. Sooting Measurement by Light Extinction. In this study, we apply the Bouguer–Beer–Lambert theory that shows the integrated sooting volume fraction for the Rayleigh scattering limitation through from equation:^{18,19}

$$f_v = \frac{\lambda \ln\left(\frac{I}{I_0}\right)}{6\pi L I_m \left\{ \frac{m^2 - 1}{m^2 + 2} \right\}} \quad (1)$$

where f_v is the integrated sooting volume fraction; λ is the incident light's wavelength; I and I_0 are respectively the intensities of transmitted and incident light; L is the absorption path length; I_m is the complex number's imaginary part; and $m = (n - ik)$ is particle's complex refractive index, and the real and imaginary values of m are expressed by n and k , respectively. The results of Dalzell's study,²⁰ $m = 1.57 - 0.51i$, were utilized to calculate sooting formation in the current investigations.

The total sooting volume which was generated within the volume of visible flame was determined by applying the expression:^{18,19}

$$V_s = \int_0^{H_f} dz \int_0^R 2\pi f_v(z, r) r dr \quad (2)$$

where V_s is the total sooting volume; H_f is the height of the visible flame; and R is the flame envelope's radius height z .

2.4. Materials. Figure 3 depicts the production process proposed in our previous study¹⁷ to create the bioparaffins

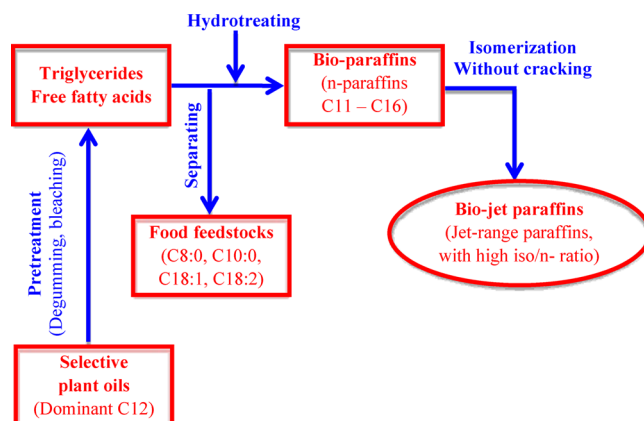


Figure 3. Route of the production process of biojet paraffins.

employed in this research. It is based on the hydrotreating process, and the medium-chain and dominating lauric (with a carbon number of 12C) fatty acids must be chosen as feedstocks. Then, the process eliminates the cracking step, using simple production technology, which reduces investment and production costs. These advantages are ideally suited to the conditions of tropical countries. In this work, the bioparaffins are made using coconut as the feedstock. The compositions of coconut oils with the primary lauric fatty acids are shown in Table 4.

The saturated fatty acids, which are primarily C_{12} – C_{16} , found in coconut oil are hydrotreated to create C_{11} – C_{16} straight-chain bioparaffins with undecane ($n-C_{11}H_{24}$) and dodecane ($n-C_{12}H_{26}$) as the main components. Figure 4 shows the chemical processes transforming lauric oil and triglyceride into undecane and dodecane.

The bioparaffins were produced by Pertamina Company, Indonesia, based on the abovementioned process. The bioparaffins have expectantly negligible aromatic content, dominant bioparaffinic compound, perhaps a little oxygenate remainders, and a tiny quantity of components with distillation temperature exceeding the ASTM requirement. The commercial Jet A1 also was supplied by the Pertamina Company. The mixture of 95% Jet A1 and 5% bioparaffins by volume, known as BK-5, was made for testing. The typical properties and their test method of bioparaffins, Jet A1, and BK-5 are presented in Table 5, in which almost BK-5 key specifications meet the criteria of ASTM-D1655.

3. RESULTS AND DISCUSSION

3.1. Effects of Brake-Specific Fuel Consumption (BSFC). The comparison of BSFC for BK-5 and Jet A1 is reported in Figure 5, which shows no apparent distinction between Jet A1 and its blend with 5% vol bioparaffins. A similar fuel consumption per unit of power produced can be attributed to no significant difference from their lower calorific value (about 0.3%). It implies an important role of specific energy in engine performances.

Table 4. Fatty Acid Compositions of Coconut Oil

| oils or fats | fatty acid compositions (% weight) | | | | | | | | |
|-----------------------|------------------------------------|---------|-------|---------|----------|-------|-------|-------|-------|
| | C8:0 | C10:0 | C12:0 | C14:0 | C16:0 | C18:0 | C18:1 | C18:2 | C18:3 |
| coconut ²¹ | 7–9 | 5–10 | 46–47 | 17–20 | 9–10 | 3 | 7–8 | 2 | |
| coconut ²² | 4.6–9.5 | 4.5–9.7 | 44–51 | 13–20.6 | 7.5–10.5 | 1–3.5 | 5–8.2 | 1–2.6 | 0–0.2 |

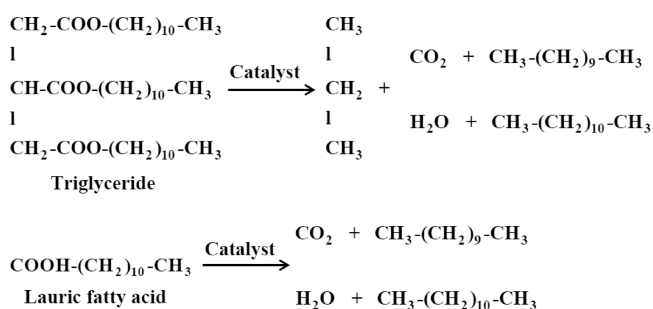
Figure 4. Chemical reaction steps for creating undecane ($n\text{-C}_{11}\text{H}_{24}$) and dodecane ($n\text{-C}_{12}\text{H}_{26}$).

Table 5. Typical Properties of Bioparaffins, Jet A1, and BK-5

| specifications | ASTM-D1655 ²³ | bioparaffins | BK-5 | Jet A1 | test method |
|---------------------------------------|--------------------------|--------------|---------|---------|-------------|
| distillation | | | | | ASTM D86 |
| initial B.P. (°C) | <Report> | 141.3 | 145.2 | 146.0 | |
| 10% Rec. (°C) | Max. 205 | 190.6 | 165.1 | 164.0 | |
| 50% Rec. (°C) | <Report> | 218.4 | 188.6 | 187.0 | |
| 90% Rec. (°C) | <Report> | 283.2 | 217.4 | 214.0 | |
| final B.P. (°C) | Max. 300 | 308.2 | 249.1 | 247.0 | |
| specific energy (MJ/kg) | Min. 42.80 | 42.48 | 44.32 | 44.45 | ASTM D4809 |
| freezing point (°C) | Max. -47.0 | 9.5 | -47.5 | -55.0 | ASTM D2386 |
| flash point (°C) | Min. 38.0 | 47.0 | 48.0 | 48.0 | ASTM D56 |
| density (kg/m ³) at 15 °C | 775–840 | 759 | 780 | 781 | ASTM D4052 |
| viscosity (cSt) at -20 °C | Max. 8.0 | | 6.94 | 6.49 | ASTM D445 |
| viscosity (cSt) at 25 °C | | 4.20 | 1.65 | 1.60 | ASTM D445 |
| sulfur, total, (wt %) | Max. 0.3 | 11 ppm | 447 ppm | 470 ppm | ASTM D4294 |

3.2. Effects of NO_x Emission. Figure 6 shows NO_x emission, TITs, and EGTs versus brake power for BK-5 and Jet A1. It is evident that the TIT, EGT, and their differences increased with increasing engine load, which agrees with that the higher power the engine operates, the higher efficiency it produces, or less fuel it consumes. Jet A1 had a higher TIT and EGT than BK-5. It may be mainly due to the aromatic concentration of Jet A1 being higher than that of its counterpart.²⁴

NO_x emissions of BK-5 were initially lower than those of Jet A1. NO_x concentrations of both fuels increased with the increasing load, but BK-5 had a larger increment than its counterpart. Eventually, NO_x emissions of BK-5 tended to be higher than those obtained with Jet A1 in the high load range. When considering the whole examined power range, BK-5 releases NO_x at a rate that is 3.4% greater than Jet A1.

In general, NO_x emissions primarily depend on the flame structure, combustion temperature, combustion mixture ratio, and the time spent at high temperatures.²⁵ In the low loads, the

higher NO_x emissions of Jet A1 may be mainly because of higher temperatures in the combustion zone of the chamber. A larger amount of fuel was injected into the combustor in the high load range. BK-5 produced bigger fuel droplet sizes, and its flames moved further downstream because of higher momentum on account of the higher viscosity of BK-5 against Jet A1. As a result, BK-5 had a longer residence time at high temperatures, a shorter combustion duration, and a higher local peak of temperature than its counterpart; this possibly is attributed to promoted thermal NO_x for BK-5 at the high loads.

3.3. Effects of CO Emission. CO emissions versus brake power for BK-5 and Jet A1 are presented in Figure 7. Conventionally, NO_x and CO emissions are trade-offs with each other. This trend, however, did not occur in this study. CO emissions of BK-5 were less than those of Jet A1 in the low-load range. This is because bioparaffins and a small amount of oxygenates improved complete combustion. In the high loads, BK-5 produced higher CO emissions than its counterpart. It may be attributed to the high-distillation temperature components in bioparaffins increased by raising fuel injected into the engine. BK-5 generated CO lower than Jet A1 by 1.8% across the evaluated power range.

3.4. Effects of HC Emission. It can be seen from Figure 8, which shows HC emission plotted along with brake power for BK-5 and Jet A1, that BK-5 had fewer HC emissions than Jet A1 in the low brake powers. It is due to the same reason related to compositions of bioparaffins which produced better combustion. With increasing power, a larger amount of the high-distillation components of bioparaffins was injected into the combustion chamber, which is a possible explanation for a slightly higher HC concentration of BK-5 against its counterpart in the middle range of power. With further increasing brake power, lower HC emissions again pertained to BK-5. It may be because BK-5 easily undergoes pyrolysis in the primary zone of the combustion chamber because of its temperature peaks being higher than those of Jet A1 in the high range of brake power, as explained above with NO_x emission. Throughout the whole power range under investigation, BK-5 produced 4.5% HC less than its counterpart.

3.5. Effects of Soot Formation in Diffusion Flames. Figure 9 presents the correlation between FMCR and flame height for BK-5 and Jet A1. The flame height and FMCR relationships of Jet A1 and its counterpart were not linear functions expressed in diffusion flame theory.^{26,27} The results, however, agreed with the work of Roper et al.²⁸ and our previous study.¹⁸ This phenomenon is attributed to the high amount of aromatic in Jet A1, which leads to high soot concentration, and an increase in the length of the soot oxidation region in the flame, resulting in a massive rise in the visible flame length.

Figures 10 and 11 present TSV plotted respectively against flame height and FMCR for BK-5 and Jet A1. In the very low range of flame heights and FMCRs, the TSVs of BK-5 were higher than those of its counterpart. In contrast, Jet A1 produced greater soot than BK-5 at the high flame height and FMCR. This phenomenon occurs due to the presence of oxygenates in the

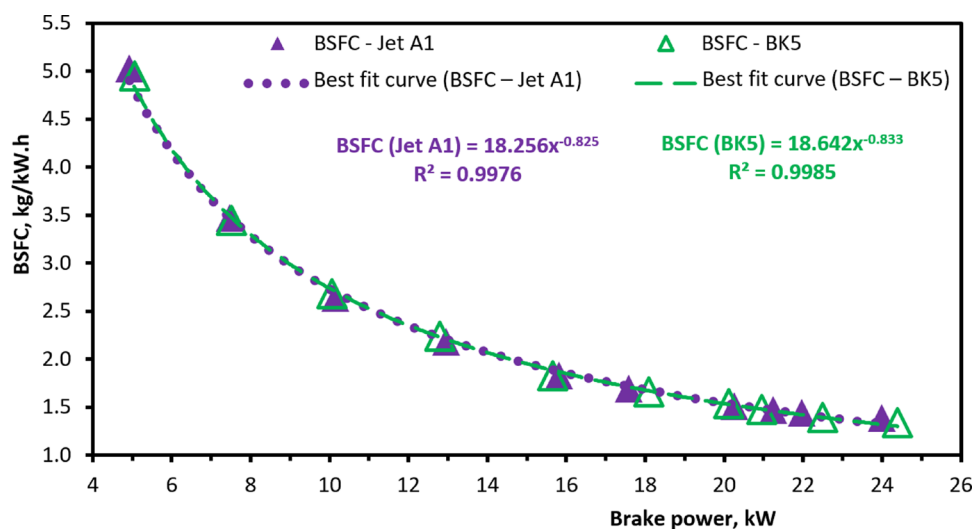


Figure 5. BSFC versus brake power for BK-5 and Jet A1.

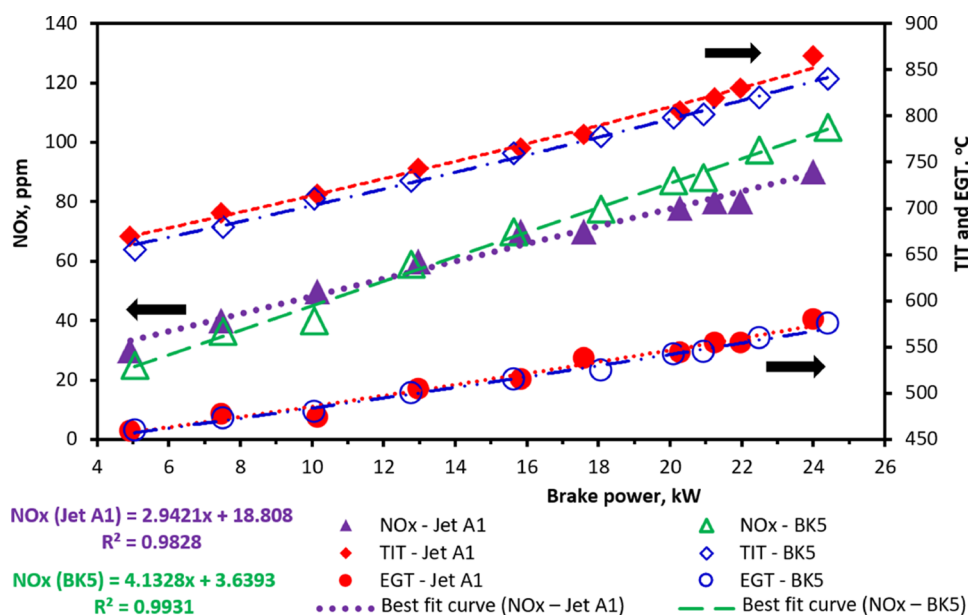


Figure 6. NO_x emission, TIT, and EGT versus brake power for BK-5 and Jet A1.

aviation bioparaffins from incomplete reactions in the manufacturing process.

When oxygen is added to fuel, there are two counteracting chemical influences on the sooting tendency in the diffusion flame.²⁹ Fuel pyrolysis is enhanced by oxygen, which promotes soot production. The radicals of aromatics and aliphatic hydrocarbons, on the other hand, are eliminated by interactions with oxygen. The net chemical effect is the difference between these two opposing influences. Both of these effects occurred at the same time in the studies of Gülder,²⁹ Wright,³⁰ Hura and Glassman,³¹ and Du et al.,³² and our previous study.¹⁸

In the low range of FMCR, the pyrolysis region was dominant in the height of flame against the burn-out zone, and the oxygenate-promoted fuel pyrolysis resulted in TSVs of BK-5 greater than those of Jet A1. In contrast, rising FMCR caused increased flame temperature; the temperature peaks and the soot volume fraction tended to move toward the burner tip. Thus, the pyrolysis region was shortened, and the oxidation zone became dominant in the flame height. Furthermore, increasing

temperature caused by increasing FMCR reduced the temperature difference by the effect of oxygen addition on the pyrolysis zone while promoting the combustion of soot in the oxidation zone. Consequently, the TSVs of BK-5 were less than those of its counterpart in the high range of FMCR. However, soot emissions from the BK-5 and Jet A1 are comparable across the thoroughly evaluated FMCR range.

4. CONCLUSIONS

We compared performances and emissions of Rove 1S/60 turbine engine burning commercial Jet A1 and its blend with 5% by volume aviation bioparaffins (BK-5). In addition, soot characteristics of diffusion flames were also observed for these two tested fuels. The following are the main conclusions from this study:

There was similar fuel consumption per unit power output between Jet A1 and BK-5. Throughout the whole power range under investigation, BK-5 emitted 3.4% NO_x higher than Jet A1, while Jet A1 released CO and HC at the rates that are

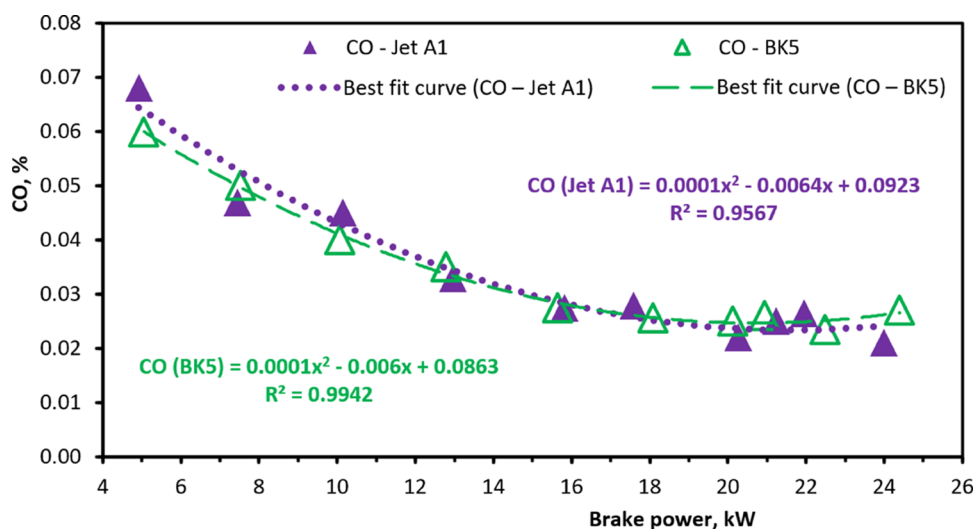


Figure 7. CO emission versus brake power for BK-5 and Jet A1.

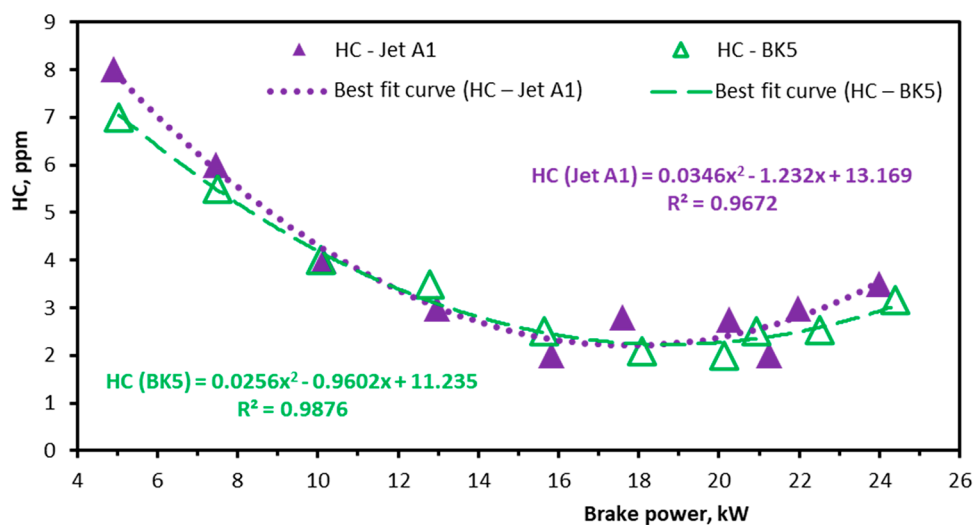


Figure 8. HC emission versus brake power for BK-5 and Jet A1.

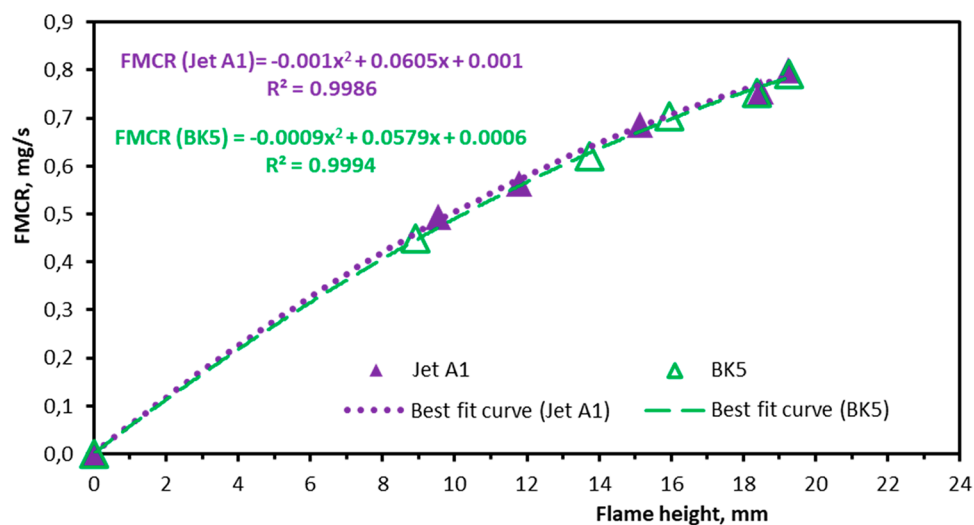


Figure 9. Correlation between FMCR and flame height for BK-5 and Jet A1.

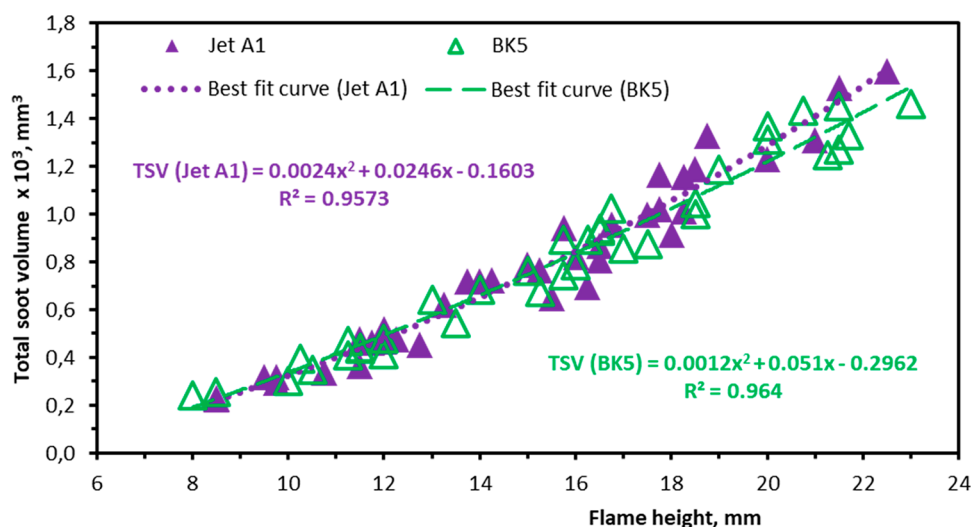


Figure 10. Correlation between the TSV and flame height for BK-5 and Jet A1.

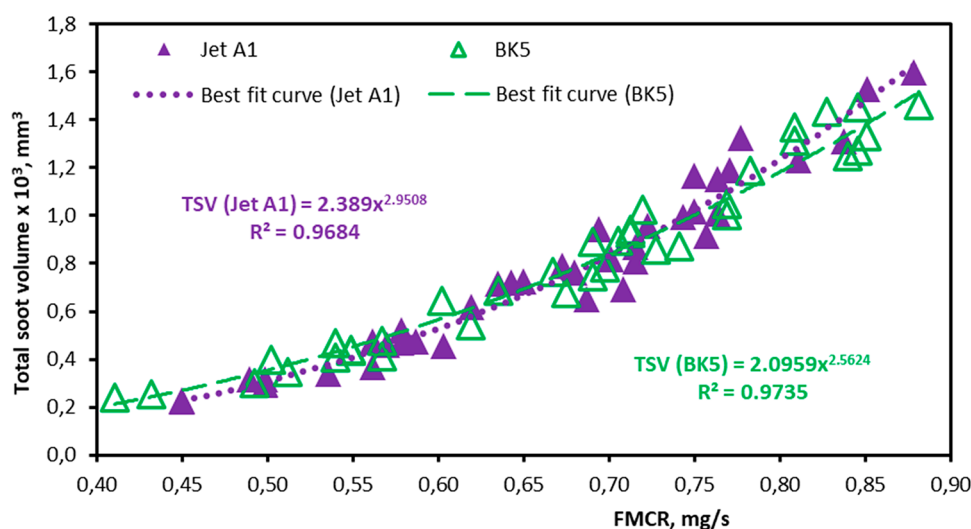


Figure 11. Correlation between the TSV and FMCR for BK-5 and Jet A1.

respectively 1.8 and 4.5% greater than its counterpart. The soot emissions from the BK-5 and Jet A1 are comparable across the measured FMCR range.

The differences in obtained emissions data between Jet A1 and BK-5 were mainly due to the higher viscosity and the composition of aviation bioparaffins, which existed with negligible aromatic content, dominant bioparaffinic compound, a small amount of oxygenates, and high-distillation temperature components. All these factors simultaneously affected the engine combustion with various levels depending on load operations and fuel consumption. The net obtained influence on emissions of a gas turbine engine is the sum of the individual effects.

Nowadays, the combustion chamber designs with low emissions tend to reduce resident time at high temperatures and premixed lean combustion through optimized mixing of liner air and enhanced fuel injection.²⁵ On this basis, the higher NO_x emissions of BK-5 in this study are considerably diminished in modern aircraft engines.

The production process of aviation biofuel, which has the most current straightforward production technology, with the feedstock of coconut oil, has been proven feasible and suitable for developing countries in the tropics.

In summary, it may be concluded that the BK-5 produced similar performance and comparable emissions and soot production against Jet A1, indicating the promising potential of aviation bioparaffins. The results motivate future studies to carry out the modern engine and flight tests. The production process should also continue to be improved by eliminating high-distillation temperature components in bioparaffins.

AUTHOR INFORMATION

Corresponding Author

Thong D. Hong – Faculty of Transportation Engineering, Ho Chi Minh City University of Technology (HCMUT), Ho Chi Minh City 700000, Vietnam; Vietnam National University Ho Chi Minh City (VNU-HCM), Ho Chi Minh City 700000, Vietnam; orcid.org/0000-0002-8010-5851; Email: hongducthong@hcmut.edu.vn

Authors

Iman K. Reksowardojo – Combustion Engines and Propulsion Systems Laboratory, Faculty of Mechanical and Aerospace Engineering, Institut Teknologi Bandung, Bandung 40132, Indonesia

Tatang H. Soerawidjaja – Department of Chemical Engineering, Faculty of Industrial Technology, Institut Teknologi Bandung, Bandung 40132, Indonesia

Osamu Fujita – Division of Mechanical and Space Engineering, Hokkaido University, Sapporo 060-8628, Japan

Complete contact information is available at:

<https://pubs.acs.org/10.1021/acsomega.2c02703>

Notes

The authors declare no competing financial interest.

ACKNOWLEDGMENTS

The Japan International Cooperation Agency (JICA) funded this study through the project of the ASEAN University Network/Southeast Asia Engineering Education Development Network (AUN/SEED-Net). The authors thank Pertamina Company, Indonesia, for supplying aviation bioparaffins.

NOMENCLATURE

Symbols

| | |
|--------------|-------------------------------|
| I | transmitted light intensity |
| I_0 | incident light intensity |
| L | absorption path length |
| λ | incident light wavelength |
| $m = n - ki$ | soot complex refractive index |
| f_v | soot volume fraction |
| V_s | total soot volume |
| H_f | flame height |
| R | radius of flame |

Abbreviations

| | |
|------|---------------------------------|
| AIT | air inlet temperature |
| TIT | turbine inlet temperature |
| EGT | exhaust gas temperature |
| TSV | total soot volume |
| FMCR | fuel mass consumption rate |
| BSFC | brake-specific fuel consumption |

Subscripts

| | |
|-----|--------|
| v | volume |
| f | flame |
| s | soot |

REFERENCES

- (1) European Parliament. Directive 2008/101/EC of the European Parliament and of the Council of 19 November 2008 Amending Directive 2003/87/EC so as to Include Aviation Activities in the Scheme for Greenhouse Gas Emission Allowance Trading within the Community. *Off. J. Eur. Union* **2009**, *L*, 3–21.
- (2) Liu, S.; Zhu, Q.; Guan, Q.; He, L.; Li, W. Bio-Aviation Fuel Production from Hydroprocessing Castor Oil Promoted by the Nickel-Based Bifunctional Catalysts. *Bioresour. Technol.* **2015**, *183*, 93–100.
- (3) Tian, Q.; Qiao, K.; Zhou, F.; Chen, K.; Wang, T.; Fu, J.; Lu, X.; Ouyang, P. Direct Production of Aviation Fuel Range Hydrocarbons and Aromatics from Oleic Acid without an Added Hydrogen Donor. *Energy Fuels* **2016**, *30*, 7291–7297.
- (4) Wang, M.; Nie, K.; Cao, H.; Xu, H.; Fang, Y.; Tan, T.; Baeyens, J.; Liu, L. Biosynthesis of Medium Chain Length Alkanes for Bio-Aviation Fuel by Metabolic Engineered *Escherichia Coli*. *Bioresour. Technol.* **2017**, *239*, 542–545.
- (5) Gutiérrez-Antonio, C.; Soria Ornelas, M. L.; Gómez-Castro, F. I.; Hernández, S. Intensification of the Hydrotreating Process to Produce Renewable Aviation Fuel through Reactive Distillation. *Chem. Eng. Process. Process Intensif.* **2018**, *124*, 122–130.
- (6) Araújo, P. H. M.; Maia, A. S.; Cordeiro, A. M. T. M.; Gondim, A. D.; Santos, N. A. Catalytic Deoxygenation of the Oil and Biodiesel of Licuri (*Syagrus Coronata*) to Obtain n-Alkanes with Chains in the Range of Biojet Fuels. *ACS Omega* **2019**, *4*, 15849–15855.
- (7) Duong, L. H.; Reksowardojo, I. K.; Soerawidjaja, T. H.; Fujita, O.; Neonufa, G. F.; Nguyen, T. T. G.; Prakoso, T. Soap-Derived Biokerosene as an Aviation Alternative Fuel: Production, Composition, and Properties of Various Blends with Jet Fuel. *Chem. Eng. Process. - Process Intensif.* **2020**, *153*, No. 107980.
- (8) da Silva, J. Q.; Santos, D. Q.; Fabris, J. D.; Harter, L. V. L.; Chagas, S. P. Light Biodiesel from Macaúba and Palm Kernel: Properties of Their Blends with Fossil Kerosene in the Perspective of an Alternative Aviation Fuel. *Renewable Energy* **2020**, *151*, 426–433.
- (9) Fu, J.; Summers, S.; Morgan, T. J.; Turn, S. Q.; Kusch, W. Fuel Properties of Pongamia (*Milletia Pinnata*) Seeds and Pods Grown in Hawaii. *ACS Omega* **2021**, *6*, 9222–9233.
- (10) Donoso, D.; Ballesteros, R.; Bolonio, D.; García-Martínez, M. J.; Lapuerta, M.; Canoira, L. Hydrogenated Turpentine: A Biobased Component for Jet Fuel. *Energy Fuels* **2021**, *35*, 1465–1475.
- (11) Li, Z.; Li, Q.; Wang, Y.; Zhang, J.; Wang, H. Synthesis of High-Density Aviation Biofuels from Biomass-Derived Cyclopentanone. *Energy Fuels* **2021**, *35*, 6691–6699.
- (12) ASTM D4054-19. *Standard Practice for Evaluation of New Aviation Turbine Fuels and Fuel Additives*; ASTM International: West Conshohocken, PA, USA, 2019.
- (13) Duong, L. H.; Fujita, O.; Reksowardojo, I. K.; Soerawidjaja, T. H.; Neonufa, G. F. Experimental Investigation of the Effects of Cycloparaffins and Aromatics on the Sooting Tendency and the Freezing Point of Soap-Derived Biokerosene and Normal Paraffins. *Fuel* **2016**, *185*, 855–862.
- (14) Kumal, R. R.; Liu, J.; Gharpure, A.; Vander Wal, R. L.; Kinsey, J. S.; Giannelli, B.; Stevens, J.; Leggett, C.; Howard, R.; Forde, M.; Zelenyuk, A.; Suski, K.; Payne, G.; Manin, J.; Bachalo, W.; Frazee, R.; Onasch, T. B.; Freedman, A.; Kittelson, D. B.; Swanson, J. J. Impact of Biofuel Blends on Black Carbon Emissions from a Gas Turbine Engine. *Energy Fuels* **2020**, *34*, 4958–4966.
- (15) Andrade-Eiroa, A.; Dagaut, P.; Dayma, G. Polar Aromatic Compounds in Soot from Premixed Flames of Kerosene, Synthetic Paraffinic Kerosene, and Kerosene-Synthetic Biofuels. *Energy Fuels* **2021**, *35*, 11427–11444.
- (16) Chang, D.; Li, J.; Yang, Y.; Gan, Z. Soot Morphology and Nanostructure Differences between Chinese Aviation Kerosene and Algae-Based Aviation Biofuel in Free Jet Laminar Diffusion Flames. *ACS Omega* **2022**, *7*, 11560–11569.
- (17) Hong, T. D.; Soerawidjaja, T. H.; Reksowardojo, I. K.; Fujita, O.; Duniani, Z.; Pham, M. X. A Study on Developing Aviation Biofuel for the Tropics: Production Process-Experimental and Theoretical Evaluation of Their Blends with Fossil Kerosene. *Chem. Eng. Process. Process Intensif.* **2013**, *74*, 124–130.
- (18) Hong, T. D.; Fujita, O.; Soerawidjaja, T. H.; Reksowardojo, I. K. Soot Formation of Dodecane, Aviation Bio-Paraffins and Their Blends with Propylbenzene in Diffusion Flames. *Renew. Energy* **2019**, *136*, 84–90.
- (19) Zelepouga, S. A.; Saveliev, A. V.; Kennedy, L. A.; Fridman, A. A. Relative Effect of Acetylene and PAHs Addition on Soot Formation in Laminar Diffusion Flames of Methane with Oxygen and Oxygen-Enriched Air. *Combust. Flame* **2000**, *122*, 76–89.
- (20) Dalzell, W. H.; Sarofim, A. F. Optical Constants of Soot and Their Application to Heat Flux Calculations. *J. Heat Transfer* **1969**, *91*, 100–104.
- (21) Mittelbach, M.; Remschmidt, C. *Biodiesel—The Comprehensive Handbook*, first ed.; Printed and Bound by Boersedruck Ges.m.b.H: Vienna, Austria, 2004.
- (22) Knothe, G.; Gerpen, J. V.; Krahl, J. *The Biodiesel Handbook*; AOCS Press: Illinois, American, 2005.
- (23) ASTM D1655-19a. *Standard Specification for Aviation Turbine Fuels*; ASTM International: West Conshohocken, PA, USA, 2019.

(24) Glaude, P. A.; Fournet, R.; Bounaceur, R.; Molière, M. Adiabatic Flame Temperature from Biofuels and Fossil Fuels and Derived Effect on NO_x Emissions. *Fuel Process. Technol.* **2010**, *91*, 229–235.

(25) Borman, G. L.; Ragland, K. W. *Combustion Engineering*. International ed.; McGraw – Hill: Singapore, 1998.

(26) Burke, S. P.; Schumann, T. E. W. Diffusion Flames. *Proc. Symp. Combust.* **1948**, *1–2*, 2–11.

(27) Roper, F. G. The Prediction of Laminar Jet Diffusion Flame Sizes: Part I. Theoretical Model. *Combust. Flame* **1977**, *29*, 219–226.

(28) Roper, F. G.; Smith, C.; Cunningham, A. C. The Prediction of Laminar Jet Diffusion Flame Sizes: Part II. Experimental Verification. *Combust. Flame* **1977**, *29*, 227–234.

(29) Gülder, Ö. L. Effects of Oxygen on Soot Formation in Methane, Propane, and n-Butane Diffusion Flames. *Combust. Flame* **1995**, *101*, 302–310.

(30) Wright, F. J. Effect of Oxygen on the Carbon-Forming Tendencies of Diffusion Flames. *Fuel* **1974**, *53*, 232–235.

(31) Hura, H. S.; Glassman, I. Soot Formation in Diffusion Flames of Fuel/Oxygen Mixtures. *Symp. Combust.* **1989**, *22*, 371–378.

(32) Du, D. X.; Axelbaum, R. L.; Law, C. K. The Influence of Carbon Dioxide and Oxygen as Additives on Soot Formation in Diffusion Flames. *Symp. Combust.* **1991**, *23*, 1501–1507.